Erythrocyte Sedimentation: Collapse of a High-Volume-Fraction Soft-Particle Gel

Alexis Darras,[1,*] Anil Kumar Dasanna,[2] Thomas John,[1] Gerhard Gompper,[2] Lars Kaestner,[1,3] Dmitry A. Fedosov,[2] and Christian Wagner[1,4]

[1]*Experimental Physics, Saarland University, 66123 Saarbruecken, Germany*

[2]*Theoretical Physics of Living Matter, Institute of Biological Information Processing and Institute for Advanced Simulation, Forschungszentrum Jülich, 52425 Jülich, Germany*

[3]*Theoretical Medicine and Biosciences, Saarland University, 66424 Homburg, Germany*

[4]*Department of Physics and Materials Science, University of Luxembourg, L-1511, Luxembourg City, Luxembourg*

(Received 23 July 2021; accepted 21 January 2022; published 23 February 2022)

The erythrocyte sedimentation rate is one of the oldest medical diagnostic methods whose physical mechanisms remain debatable today. Using both light microscopy and mesoscale cell-level simulations, we show that erythrocytes form a soft-particle gel. Furthermore, the high volume fraction of erythrocytes, their deformability, and weak attraction lead to unusual properties of this gel. A theoretical model for the gravitational collapse is developed, whose predictions are in agreement with detailed macroscopic measurements of the interface velocity.

DOI: 10.1103/PhysRevLett.128.088101

The erythrocyte sedimentation rate (ESR) is one of the oldest medical diagnostic tools, with its origin rooted in ancient Greek times [1]. It was popularized in the late 19th and early 20th century as a nonspecific test to diagnose and monitor inflammation [2–4]. However, recent research has shown that it might also be a good and cheap biomarker to detect abnormal, deformed erythrocytes [or red blood cells (RBCs)] [5]. Despite its frequent use in medicine, physical mechanisms that govern the sedimentation of erythrocytes did not advance much during the last century. It is generally accepted that erythrocytes agglomerate into separate aggregates whose sedimentation is well described by a Stokes-like law [6–10]. However, the corresponding physical models for erythrocyte sedimentation are often semiempirical, and provide at best a qualitative description [8–10].

Several decades of research on the sedimentation of particles suspensions have shown that many suspensions of attractive particles form a particle gel, which sediments very differently from a collection of separate aggregates. For instance, the sedimentation of such gels is characterized by a delayed, sudden collapse, sometimes associated with the emergence of cracks within the gel structure [11–13]. These gels also exhibit a sharp interface between the free liquid phase and the gel of particles [14–17]. In this Letter, we show that this gel interpretation provides a consistent and quantitative description of the sedimentation of erythrocytes at physiological volume fractions. In particular, we show that erythrocytes form a soft gel whose sedimentation is well described by a theoretical description based on the collapse of gel-like suspensions. Furthermore, complementary simulations demonstrate that erythrocyte flexibility and high volume fraction are important parameters that determine the gel-like behavior of erythrocyte suspension (or blood) (see the companion paper [18]).

Despite the fact that ESR is often explained as the sedimentation of separate aggregates, several current studies already provide some arguments supporting the idea of gel-like sedimentation: (i) The formation of distinct aggregates of RBCs should result in a strongly polydisperse suspension [19]. Suspensions with polydisperse aggregates form a diffuse interface during sedimentation [20–22], contrary to what is observed for erythrocyte sedimentation at physiological hematocrit (volume fraction of RBCs) values of $0.35 < \phi_0 < 0.50$. (ii) Because of the low shear stress during their sedimentation, the aggregation process of erythrocytes is nearly irreversible. Such an aggregation on the timescale of minutes to hours leads to a percolating (or space-filling) network of RBCs [23]. This is consistent with a gel-like structure observed for even more dilute suspensions of other attractive particles [14]. (iii) The interface position between the dense erythrocyte phase and the free liquid (blood plasma) can actually oscillate or jump in time [24]. (iv) A notable modification in suspension conductivity has been observed for sedimenting erythrocytes, which can be explained by the opening of channels for the liquid phase, i.e., the plasma, within aggregated erythrocyte structures [25,26]. Such channels are characteristic for the sedimentation of particle gels [11].

The main reason for the so-far generally accepted picture that erythrocytes sediment as separate aggregates is that the sedimentation velocity increases with the aggregation interaction strength between erythrocytes, which is mainly determined by the concentration of polymers (and in particular fibrinogen) in the plasma [27,28]. However, previous models of gravitational collapse of particle gels

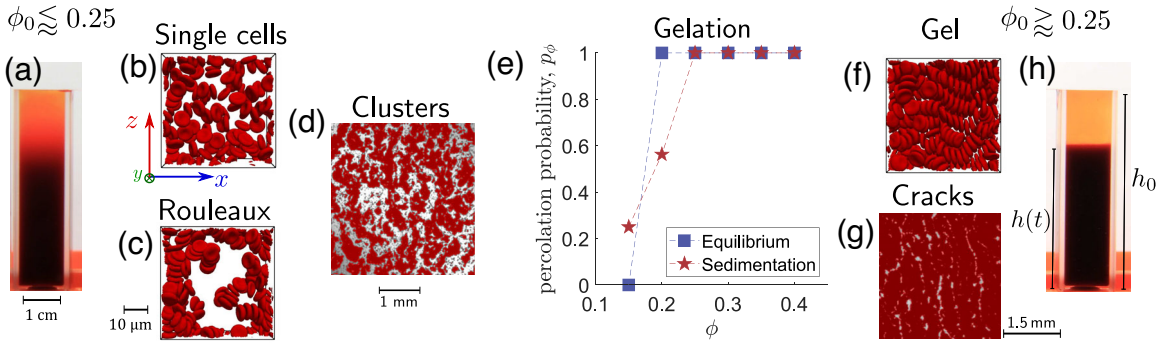

FIG. 1. Possible regimes of erythrocyte sedimentation. (a) Experimental photograph of a low volume fraction ($\phi_0 = 0.2$) erythrocyte suspension, after 20 min at rest in a cuvette with quadratic cross section. A diffuse interface hints to a sedimentation of separate aggregates. (b) Snapshot from simulation: well-dispersed suspension of erythrocytes for $\phi = 0.25$ and no attraction force between the cells. (c) Snapshot from simulation: formation of rouleaux structures at $\phi = 0.25$ and physiological attraction between the cells ($\epsilon = 2.5 k_B T$, see the companion paper for details [18]). (d) False-color photograph of erythrocytes clusters in a 150 μm thick container, at volume fraction $\phi = 0.20$ (see also Supplemental Movie S1 [42]). (e) Percolation probability p_ϕ is plotted against hematocrit ϕ (simulations have a constant hematocrit due to periodic boundary conditions on z). The probability p_ϕ is defined as the fraction of snapshots in which the largest cluster is percolating in both x and y (periodic) directions. The data are shown for both sedimentation and equilibrium. (f) A gel-like network for $\phi = 0.4$. All simulation snapshots have the same scale. (g) False-color photograph of the cracks for blood sedimentation in a 150 μm thick container, at volume fraction $\phi = 0.45$ (see also Supplemental Movie S2 [42]). (h) Erythrocyte suspension with physiological volume fraction ($\phi_0 = 0.45$), after 2 hours at rest. A sharp interface, indicating a gel-like collapse behavior, is observed.

also show that increased attraction increases the rigidity of the network and slows down the sedimentation [15,29–36]. Pribush *et al.* [25,26] mention the possibility of a transient erythrocyte gel, but claim that such a percolating network must break into separate aggregates during sedimentation due to the induced upward flow of plasma (caused by volume conservation). Furthermore, there is disagreement in how hematocrit ϕ_0 affects the ESR, where the majority of studies finds that the ESR decreases with ϕ_0 [37–39], while others support the opposite dependence [26].

To reconcile these different interpretations, we perform ESR measurements with various volume fractions in combination with 3D hydrodynamic simulations for the analysis of cell-level structure and dynamics. Sedimentation experiments are performed in cuvettes with inner dimensions of $10 \times 10 \times 40$ mm^3 to minimize wall effects on RBC sedimentation [11,15].

Blood samples were collected from various healthy volunteers with an informed consent [40]. For $\phi_0 < 0.25$, a diffuse interface between erythrocytes and plasma is observed [Fig. 1(a)], while a sharp interface is obtained at higher ϕ [Fig. 1(h)]. This suggests that a transition between the regimes of separated aggregates and soft-particle gel occurs at $\phi_0 \approx 0.25$, at otherwise physiological conditions. This is also consistent with the percolation threshold of athermal disks with similar aspect ratio reported previously in the literature [41].

We also performed experiments with a container made of two glass plates separated by a paraffin layer (around 150 μm thick, 2 cm wide, and 6 cm high). Those experiments are illustrated in Supplemental Figure S1 [42]. These containers reveal the separated microscopic aggregates (Fig. 1(d) and Supplemental Movie S1 [42]) for $\phi_0 = 0.2$ and the apparition of channels in a cohesive gel for $\phi_0 = 0.45$ (Fig. 1(g) and Movie S2 [42]). The Movie S3 [42] also shows a so-called eruption of the gel [11], which was previously hypothesized as the explanation for the fluctuations of the interface [33].

In order to gain deeper insight into the governing physical mechanisms, we also perform mesoscopic computer simulations of aggregation of deformable RBCs, with biconcave-disc shape at rest, and with short-range intercell attractive membrane interactions, combined with fluid modeled by smoothed dissipative particle dynamics [46,47]. The simulation domain is cubic with a side length $L = 50$ μm and has periodic boundary conditions in all three directions. Constant volume fractions in the range $\phi \in [0.15; 0.4]$ were probed, meaning between ~200 and 500 cells are simulated. We perform simulations in thermal equilibrium, and in a gravitational field that induces upward liquid flow. In both cases, the simulations show aggregated gel-like networks spanning the whole simulation domain; see Fig. 1(f). To check if the cluster is percolating, for our case of periodic boundary conditions, we employ periodic images of the box in the x and y directions (excluding the sedimentation direction, i.e., the z direction) and measure the cluster size in these two directions. If the cluster is percolating, the cluster size is equal to $2L$. If the cluster is not percolating, the cluster size becomes smaller than L (but is often close to L). The percolation probability is then defined as the fraction of times the largest cluster, which contains a large fraction of all cells, is percolating in both x and y directions. In Fig. 1(e), we plot the percolation probability p_ϕ for different hematocrit values for both

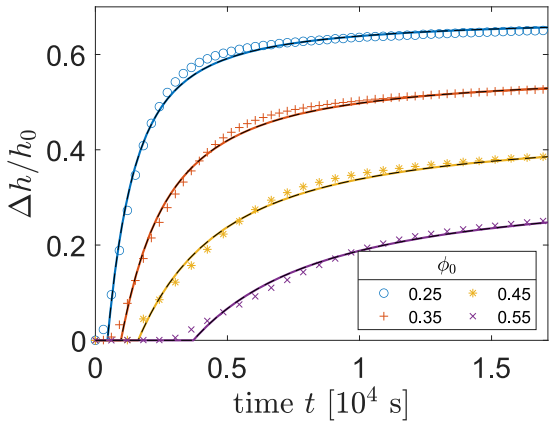

FIG. 2. Measurements of relative height reduction $\Delta h/h_0 = [h(0) - h(t)]/h(0)$ of the dense erythrocyte suspension below the free liquid phase (plasma), for various hematocrits. Note that Δh corresponds to the height of top plasma layer. The symbols are experimental data, while the curves are fits from our model for $h(t)$ from Eq. (5).

equilibrium and sedimentation. For smaller hematocrit values, the largest cluster breaks into smaller clusters representing the "fluid" state of the suspension; see Figs. 1(b),(c). For hematocrits $\phi_0 > 0.25$, the largest cluster is always percolating, in agreement with experimental observations. In the absence of sedimentation, and thus without global upward liquid flow, percolation appears for smaller hematocrit values and the percolation transition with varying volume fraction is sharp. Analysis of the erythrocytes kinetics at various hematocrits is available in the Supplemental Material [42].

Further quantitative measurements can be obtained from the experiments by focusing on the interface between the free liquid (plasma) and the dense erythrocytes suspension. Figure 2 shows the variation of this interface position and Fig. 3(a) its velocity. This interface velocity defines the sedimentation velocity, and decreases with increasing hematocrit for volume fractions $\phi_0 \gtrsim 0.25$ (physiological values range from 0.35 to 0.50 [48]). An interesting observation is that the delay time of sedimentation increases significantly with increasing ϕ_0 (see Fig. 2). This is in agreement with gels that become more stable with increasing volume fraction of attractive particles, and thus, require longer times for aging toward an eventual collapse or sedimentation start. For the sedimentation of separate aggregates, the delay time attributed to initial diffusion-limited RBC aggregation should decrease with increasing ϕ_0, because intercell distances decrease and the aggregation should proceed faster [49].

For a quantitative description of the erythrocyte sedimentation process, we develop a semiempirical model based on the collapse of a particle gel. Previous models for sedimenting gels are not suitable for blood because they consider particles with higher attraction and whose time-dependent volume fraction is assumed to be small such that $(1-\phi) \gg \phi$ [11,14,15]. For blood sedimentation, this assumption is not valid, as ϕ initially starts from about 0.4 and finishes with a value close to unity when sedimentation stops. For simplicity, we assume that the volume fraction ϕ of the erythrocyte gel phase is spatially homogeneous but time dependent. The conservation of erythrocyte volume can be expressed as $h(t)\phi(t) = \phi_0 h_0$, where $h(t)$ is the time-dependent position of the gel surface and $h_0 = h(0)$ is the initial height. Assuming a sharp interface between cell-free plasma and erythrocyte gel, total volume conservation allows the connection between $h(t)$ and v, the average (upward) velocity of the plasma at the interface,

$$(1-\phi)v + \phi\frac{dh}{dt} = 0. \tag{1}$$

Considering that pressure gradients that drive upward plasma flow develop due to the gravity force on erythrocytes, we obtain

$$-(1-\phi)\frac{\partial P}{\partial z} = \Delta\rho g\phi, \tag{2}$$

where P is the pressure, $\Delta\rho$ is the density difference between erythrocyte and plasma, and g is the gravitational acceleration. Note that other possible stresses within erythrocyte gel, such as elastic stresses, are neglected here. Indeed, the final volume fractions ϕ_m are close to their close packing fraction [50–54]. The system is then not stopped by the elasticity of the structure, but rather by the incompressibility of the single erythrocytes. Indeed, for the network elasticity to balance gravity, one would need an elastic modulus of $E \approx -\Delta\rho g\phi_m(H^2/2\Delta h) \gtrsim 10$ Pa. This modulus E is 30 to 250 times higher than the one reported in the literature from rheology (0.04 to 0.32 Pa [55,56], for $\phi \geq 0.8$) (see the Supplemental Material [42] for further justification).

Flow through a porous material is modeled by Darcy's law:

$$(1-\phi)\left(v - \frac{dh}{dt}\right) = -\frac{k}{\eta}\frac{\partial P}{\partial z}, \tag{3}$$

where k is the permeability of the medium and η is the fluid dynamic viscosity. To approximate the permeability k, we use a modified Carman-Kozeny relationship for packed beds of particles, as proposed by Terzaghi [57] and employed by others [58]:

$$k = \frac{1}{\kappa_0}\frac{a^2(\phi_m - \phi)^3}{\phi^2}, \tag{4}$$

where a is the characteristic size of medium pores, κ_0 is the scaling constant in the Carman-Kozeny relationship that depends on geometric properties of the porous medium [59–61], and ϕ_m is the maximal volume fraction at which

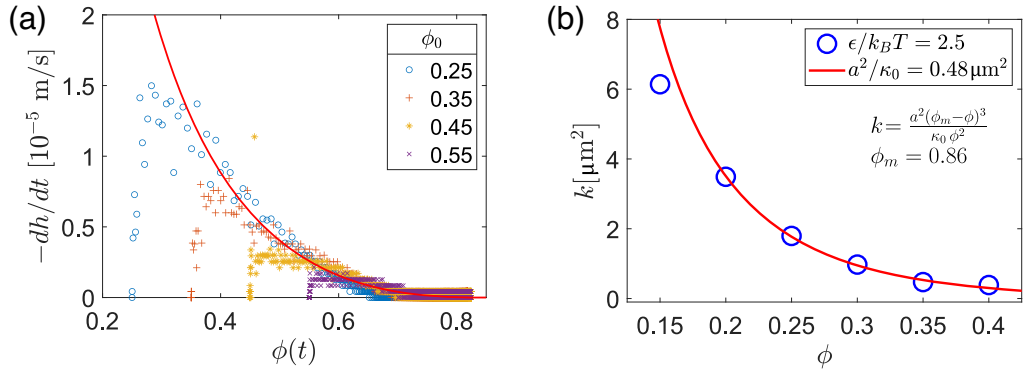

FIG. 3. Erythrocyte sedimentation for various initial volume fractions. (a) Measurements of velocity of the interface between the erythrocytes gel and the plasma (same experiments as in Fig. 2). The symbols are experimental data. The average velocity between two measurement points is dh/dt, and $\phi(t) = \phi_0 h_0/h(t)$. The solid curve is obtained from Eq. (5) using average values of $\gamma = 0.42 \pm 0.06$ and $\phi_m = 0.86 \pm 0.04$ from the entire set of measurements (16 samples from seven independent blood drawings). (b) Permeability coefficient from hydrodynamic simulations calculated as $k = (1-\phi)v\eta/(\partial P/\partial z)$ as a function of hematocrit. The assumed aggregation strength in simulations was $\epsilon = 2.5 k_B T$ (see the companion paper [18]).

liquid stops flowing through the medium. The parameter ϕ_m is a modification introduced initially for compact clay media, because at high volume fractions, the permeability can become zero even for $\phi < 1$ [58]. In the case of blood, the sedimentation process induces the compaction of erythrocyte packing, which finally stops at a maximal volume fraction $\phi_m < 1$. Interestingly, elastic gels with constant ϕ usually assume $k_0 \approx a^2/\phi^{2/(3-d)}$, with d the fractal exponent of the aggregates [14,15]. However, we show in Fig. 3(b) that Eq. (4) offers the relevant scaling.

By combining Eqs. (1) through (4), and the elimination of $\partial P/\partial z$, we obtain an equation for time evolution of the height h of erythrocyte gel as

$$\frac{dh}{dt} = -\frac{\Delta\rho g a^2}{\kappa_0 \eta}\frac{(\phi_m - \phi)^3}{\phi(1-\phi)}, \tag{5}$$

where $\phi = \phi_0 h_0/h$ due to the conservation of erythrocyte volume. Furthermore, erythrocyte sedimentation exhibits a delayed collapse as shown in Fig. 2, which is similar to particle gels. The origin of sedimentation delay is still under debate, and is likely associated with gel aging and the development of cracks for fluid to flow within the gel [12,34,62–64]. Such a delay time has already been used in an empirical model for blood sedimentation [27]. In our model, the delay time t_0 is introduced as an adjustable parameter, such that $(dh/dt) = 0$ for $t < t_0$ and erythrocyte sedimentation proceeds according to Eq. (5) for $t > t_0$.

Even though Eq. (5) does not have a direct analytical solution for $h(t)$, it was used to fit experimental sedimentation results with two additional adjustable parameters: ϕ_m and $\gamma = \kappa_0/a^2$, where the latter is related to a characteristic time in this system (see the Supplemental Material [42] and the companion paper [18] for details).

Several fits using this model are shown in Fig. 2 with a good quantitative agreement between experimental measurements and model predictions for various hematocrits. Supplemental Figure S2 [42] presents fitting parameters (γ, ϕ_m, and t_0) for all sedimentation measurements performed. The parameters γ and ϕ_m display small deviations (respectively, up to 15% and 5%) without any particular trend, indicating their robustness for the quantification of the ESR independently of hematocrit. The observed delay time t_0 is the only parameter that strongly depends on ϕ_0. This is consistent with the idea that the delay in sedimentation is related to the time required for the rearrangement of a gelated network [34,63], since a larger hematocrit implies stronger connectivity within erythrocyte gel.

Another result of our theoretical description is that the sedimentation velocity is a function of a local time-dependent hematocrit. Indeed, Fig. 3(a) compares interface velocities from Eq. (5) and experimental measurements for different ϕ_0. All collected data collapse onto a single master curve predicted by Eq. (5) with $\gamma = 0.34$ and $\phi_m = 0.86$, except a few time points collected below or around the time delay t_0. The discrepancies in sedimentation velocity at the very start of sedimentation are likely related to the time required for flow development within an erythrocyte gel.

The hydrodynamic simulations of sedimentation confirm the relevance of the model. Figure 3(b) shows the permeability coefficient k, computed through Eq. (3), as a function of hematocrit. These data are fitted with Eq. (4). The fit closely approximates the simulation data and confirms the validity of Eq. (4) as constitutive equation. Furthermore, these hydrodynamic simulations show that for large enough $\phi_0 > 0.25$, even though some rearrangements in the gel-like erythrocyte network occur due to sedimenting flow conditions, it still spans the whole simulation domain. Thus, it indicates that for physiological hematocrit values, the initially gelated structure of RBCs

likely does not break into separate aggregates during the sedimentation process.

In summary, we have shown that erythrocyte suspensions sediment as a soft particle gel when the physiological range of hematocrits is considered. The developed theoretical model is able to quantitatively describe the behavior of the interface of the erythrocytes gel under conditions relevant for the usual clinical tests. Numerical simulations corroborate the robustness of the theoretical model for erythrocyte sedimentation, and confirm that at physiological hematocrit values, a gel-like network structure of erythrocytes remains even under sedimenting flow conditions. This sedimentation corresponds to a sudden collapse of the gel when it fractures and condenses. The companion paper [18] presents a systematic investigation of the effect of aggregation strength between erythrocytes on the interface velocity. Our study provides a significant step toward understanding erythrocyte sedimentation employed in classical ESR tests, but also provides a theoretical background for changes in erythrocyte sedimentation related to some diseases (e.g., acanthocytosis), in which erythrocyte properties might be significantly altered [5].

This work was supported by the research unit FOR 2688 - Wa1336/12 of the German Research Foundation, and by the Marie Skłodowska-Curie grant agreement No. 860436—EVIDENCE. T. J. and C. W. acknowledge funding from French German University (DFH/UFA). We gratefully acknowledge the computing time granted through JARA-HPC on the supercomputer JURECA at Forschungszentrum Jülich.

*Corresponding author.
alexis.charles.darras@gmail.com

[1] I. Kushner, The acute phase response: An overview, Methods Enzymol. **163**, 373 (1988).
[2] A. Grzybowski and J. Sak, Edmund biernacki (1866-1911): Discoverer of the erythrocyte sedimentation rate. On the 100th anniversary of his death, Clin. Dermatol. **29**, 697 (2011).
[3] S. E. Bedell and B. T. Bush, Erythrocyte sedimentation rate. From folklore to facts, Am. J. Med. **78**, 1001 (1985).
[4] K. Tishkowski and V. Gupta, Erythrocyte sedimentation rate (esr), in *StatPearls [PMID: 32491417]* (StatPearls Publishing, Treasure Island, 2020).
[5] A. Darras, K. Peikert, A. Rabe, F. Yaya, G. Simionato, T. John, A. K. Dasanna, S. Buvalyy, J. Geisel, A. Hermann *et al.*, Acanthocyte sedimentation rate as a diagnostic biomarker for neuroacanthocytosis syndromes: Experimental evidence and physical justification, Cells **10**, 788 (2021).
[6] M. A. Taye, Sedimentation rate of erythrocyte from physics prospective, Eur. Phys. J. E **43**, 19 (2020).
[7] R. Smallwood, W. Tindale, and E. Trowbridge, The physics of red cell sedimentation, Phys. Med. Biol. **30**, 125 (1985).
[8] C. Puccini, D. Stasiw, and L. Cerny, The erythrocyte sedimentation curve: A semi-empirical approach, Biorheology **14**, 43 (1977).
[9] K. L. Dorrington and B. S. Johnston, The erythrocyte sedimentation rate time curve: Critique of an established solution, J. Biomech. **16**, 99 (1983).
[10] J. V. d. C. Sousa, M. N. dos Santos, L. Magna, and E. C. de Oliveira, Validation of a fractional model for erythrocyte sedimentation rate, Comput. Appl. Math. **37**, 6903 (2018).
[11] C. Derec, D. Senis, L. Talini, and C. Allain, Rapid settling of a colloidal gel, Phys. Rev. E **67**, 062401 (2003).
[12] P. Bartlett, L. J. Teece, and M. A. Faers, Sudden collapse of a colloidal gel, Phys. Rev. E **85**, 021404 (2012).
[13] W. C. Poon, L. Starrs, S. Meeker, A. Moussaid, R. M. Evans, P. Pusey, and M. Robins, Delayed sedimentation of transient gels in colloid–polymer mixtures: Dark-field observation, rheology and dynamic light scattering studies, Faraday Discuss. **112**, 143 (1999).
[14] C. Allain, M. Cloitre, and M. Wafra, Aggregation and Sedimentation in Colloidal Suspensions, Phys. Rev. Lett. **74**, 1478 (1995).
[15] S. Manley, J. M. Skotheim, L. Mahadevan, and D. A. Weitz, Gravitational Collapse of Colloidal Gels, Phys. Rev. Lett. **94**, 218302 (2005).
[16] P. Padmanabhan and R. Zia, Gravitational collapse of colloidal gels: Non-equilibrium phase separation driven by osmotic pressure, Soft Matter **14**, 3265 (2018).
[17] J. Rouwhorst, P. Schall, C. Ness, T. Blijdenstein, and A. Zaccone, Nonequilibrium master kinetic equation modeling of colloidal gelation, Phys. Rev. E **102**, 022602 (2020).
[18] A. K. Dasanna, A. Darras, T. John, G. Gompper, L. Kaestner, C. Wagner, and D. A. Fedosov, companion paper, Erythrocyte sedimentation: Effect of aggregation energy on gel structure during collapse, Phys. Rev. E **105**, 024610 (2022).
[19] R. B. Ami, G. Barshtein, D. Zeltser, Y. Goldberg, I. Shapira, A. Roth, G. Keren, H. Miller, V. Prochorov, A. Eldor *et al.*, Parameters of red blood cell aggregation as correlates of the inflammatory state, Am. J. Physiol.-Heart Circ. Physiol. **280**, H1982 (2001).
[20] B. Xue and Y. Sun, Modeling of sedimentation of polydisperse spherical beads with a broad size distribution, Chem. Eng. Sci. **58**, 1531 (2003).
[21] A. D. Watson, G. C. Barker, and M. M. Robins, Sedimentation in bidisperse and polydisperse colloids, J. Colloid Interface Sci. **286**, 176 (2005).
[22] M. Selim, A. Kothari, and R. Turian, Sedimentation of multisized particles in concentrated suspensions, Am. Instit. Chem. Eng. J. **29**, 1029 (1983).
[23] A. Pribush, H. Meiselman, D. Meyerstein, and N. Meyerstein, Dielectric approach to investigation of erythrocyte aggregation. II. Kinetics of erythrocyte aggregation–disaggregation in quiescent and flowing blood, Biorheology **37**, 429 (2000).
[24] V. V. Tuchin, X. Xu, and R. K. Wang, Dynamic optical coherence tomography in studies of optical clearing, sedimentation, and aggregation of immersed blood, Appl. Opt. **41**, 258 (2002).

[25] A. Pribush, D. Meyerstein, and N. Meyerstein, The mechanism of erythrocyte sedimentation. Part 1: Channeling in sedimenting blood, Colloids Surf. B **75**, 214 (2010).
[26] A. Pribush, D. Meyerstein, and N. Meyerstein, The mechanism of erythrocyte sedimentation. Part 2: The global collapse of settling erythrocyte network, Colloids Surf. B **75**, 224 (2010).
[27] W. Hung, A. Collings, and J. Low, Erythrocyte sedimentation rate studies in whole human blood, Phys. Med. Biol. **39**, 1855 (1994).
[28] L. Holley, N. Woodland, W. T. Hung, K. Cordatos, and A. Reuben, Influence of fibrinogen and haematocrit on erythrocyte sedimentation kinetics, Biorheology **36**, 287 (1999).
[29] G. M. Channell, K. T. Miller, and C. F. Zukoski, Effects of microstructure on the compressive yield stress, AIChE J. **46**, 72 (2000).
[30] M. L. Kilfoil, E. E. Pashkovski, J. A. Masters, and D. Weitz, Dynamics of weakly aggregated colloidal particles, Phil. Trans. R. Soc. A **361**, 753 (2003).
[31] S. W. Kamp and M. L. Kilfoil, Universal behaviour in the mechanical properties of weakly aggregated colloidal particles, Soft Matter **5**, 2438 (2009).
[32] A. D. Dinsmore, V. Prasad, I. Y. Wong, and D. A. Weitz, Microscopic Structure and Elasticity of Weakly Aggregated Colloidal Gels, Phys. Rev. Lett. **96**, 185502 (2006).
[33] A. Pribush, D. Meyerstein, and N. Meyerstein, The mechanism of erythrocyte sedimentation. Part 1: Channeling in sedimenting blood, Colloids Surf. B **75**, 214 (2010).
[34] L. J. Teece, J. M. Hart, K. Y. N. Hsu, S. Gilligan, M. A. Faers, and P. Bartlett, Gels under stress: The origins of delayed collapse, Colloids Surf. A **458**, 126 (2014).
[35] S. B. Lindström, T. E. Kodger, J. Sprakel, and D. A. Weitz, Structures, stresses, and fluctuations in the delayed failure of colloidal gels, Soft Matter **8**, 3657 (2012).
[36] D. Senis, L. Talini, and C. Allain, Settling in aggregating colloidal suspensions, Oil Gas Sci. Technol. **56**, 153 (2001).
[37] J. Poole and G. Summers, Correction of ESR in anaemia, Br. Med. J. **1**, 353 (1952).
[38] B. S. Bull and G. Brecher, An evaluation of the relative merits of the wintrobe and westergren sedimentation methods, including hematocrit correction, American Journal of Clinical Pathology **62**, 502 (1974).
[39] O. Baskurt, B. Neu, and H. J. Meiselman, *Red Blood Cell Aggregation* (CRC Press, Boca Raton, 2011).
[40] According to the declaration of Helsinki and the approval by the ethics committee "rztekammer des Saarlandes," ethics votum 51/18.
[41] M. Mathew, T. Schilling, and M. Oettel, Connectivity percolation in suspensions of hard platelets, Phys. Rev. E **85**, 061407 (2012).
[42] See Supplemental Material, which includes Refs. [43–45], at http://link.aps.org/supplemental/10.1103/PhysRevLett.128.088101 for some additional details on the fitting process and descriptions of the supplemental movies and figures. The movies are as follows: Supplemental Movie S1/Hem20StartSpedUpX30.avi (Separated aggregates of erythrocytes during sedimentation at low hematocrit), Supplemental Movie S2/Hem45SpedUp150X.avi (Gel structure of erythrocytes during sedimentation for physiological hematocrit), and Supplemental Movie S3/CloseUpEruption-Hem45.avi (Close-up movie of an eruption). The figures are Supplemental Figure S1 (Various regimes of erythrocytes sedimentation observed in a narrow container) and Supplemental Figure S2 (Complete range of measured parameters for healthy donors).
[43] N. Norouzi, H. C. Bhakta, and W. H. Grover, Sorting cells by their density, PLoS One **12**, e0180520 (2017).
[44] R. J. Trudnowski and R. C. Rico, Specific gravity of blood and plasma at 4 and 37 c, Clin. Chem. **20**, 615 (1974).
[45] G. Késmárky, P. Kenyeres, M. Rábai, and K. Tóth, Plasma viscosity: A forgotten variable, Clin. Hemorheol. Microcircu. **39**, 243 (2008).
[46] D. A. Fedosov, H. Noguchi, and G. Gompper, Multiscale modeling of blood flow: From single cells to blood rheology, Biomech. Model. Mechanobiol. **13**, 239 (2014).
[47] K. Müller, D. A. Fedosov, and G. Gompper, Smoothed dissipative particle dynamics with angular momentum conservation, J. Comput. Phys. **281**, 301 (2015).
[48] C. C. Chernecky and B. J. Berger, *Laboratory Tests and Diagnostic Procedures* (Elsevier, Amsterdam, 2012).
[49] W. Russel, D. Saville, and W. Schowalter, *Colloidal Dispersions* (Cambridge University Press, Cambridge, England, 1989).
[50] H. Wensink and H. Lekkerkerker, Phase diagram of hard colloidal platelets: A theoretical account, Mol. Phys. **107**, 2111 (2009).
[51] J. G. Berryman, Random close packing of hard spheres and disks, Phys. Rev. A **27**, 1053 (1983).
[52] D. E. G. Williams, Packing fraction of a disk assembly randomly close packed on a plane, Phys. Rev. E **57**, 7344 (1998).
[53] G. Delaney, D. Weaire, S. Hutzler, and S. Murphy, Random packing of elliptical disks, Philos. Mag. Lett. **85**, 89 (2005).
[54] A. Darras, H. G. Breunig, T. John, R. Zhao, J. Koch, C. Kummerow, C. König, C. Wagner, and L. Kaestner, Imaging erythrocyte sedimentation in whole blood, Front. Physiol. **12**, 729191 (2022).
[55] R. Tran-Son-Tay, B. Coffey, and R. Hochmuth, A rheological study of packed red blood cell suspensions with an oscillating ball micro rheometer, Biorheology **26**, 143 (1989).
[56] G. Tomaiuolo, A. Carciati, S. Caserta, and S. Guido, Blood linear viscoelasticity by small amplitude oscillatory flow, Rheol. Acta **55**, 485 (2016).
[57] K. Terzaghi, *Erdbaumechanik auf bodenphysikalischer Grundlage* (F. Deuticke, Leipzig und Wien, 1925).
[58] P. C. Carman, Permeability of saturated sands, soils and clays, J. Agric. Sci. **29**, 262 (1939).
[59] T. Ozgumus, M. Mobedi, and U. Ozkol, Determination of Kozeny constant based on porosity and pore to throat size ratio in porous medium with rectangular rods, Eng. Appl. Comput. Fluid Mech. **8**, 308 (2014).
[60] A. W. J. Heijs and C. P. Lowe, Numerical evaluation of the permeability and the Kozeny constant for two types of porous media, Phys. Rev. E **51**, 4346 (1995).
[61] P. Xu and B. Yu, Developing a new form of permeability and Kozeny–Carman constant for homogeneous porous media

by means of fractal geometry, Adv. Water Resour. **31**, 74 (2008).

[62] R. Buscall, T. H. Choudhury, M. A. Faers, J. W. Goodwin, P. A. Luckham, and S. J. Partridge, Towards rationalising collapse times for the delayed sedimentation of weakly-aggregated colloidal gels, Soft Matter **5**, 1345 (2009).

[63] V. Gopalakrishnan, K. S. Schweizer, and C. Zukoski, Linking single particle rearrangements to delayed collapse times in transient depletion gels, J. Phys. Condens. Matter **18**, 11531 (2006).

[64] P. Padmanabhan and R. Zia, Gravitational collapse of colloidal gels: Non-equilibrium phase separation driven by osmotic pressure, Soft Matter **14**, 3265 (2018).